Tissue-Specific Gene Inactivation in *Xenopus laevis*: Knockout of *lhx1* in the Kidney with CRISPR/Cas9

Bridget D. DeLay,* Mark E. Corkins,* Hannah L. Hanania,*,† Matthew Salanga,‡,1 Jian Min Deng,§ Norihiro Sudou, Masanori Taira,†† Marko E. Horb,‡ and Rachel K. Miller*,§,‡‡,§§,2**

*Department of Pediatrics, Pediatric Research Center, University of Texas Health Science Center McGovern Medical School, Houston, Texas 77030, †Program in Biochemistry and Cell Biology, Rice University, Houston, Texas 77251, ‡National *Xenopus* Resource and Eugene Bell Center for Regenerative Biology and Tissue Engineering, Marine Biological Laboratory, Woods Hole, Massachusetts 02543, §Department of Genetics, University of Texas MD Anderson Cancer Center, Houston, Texas 77030, **Department of Anatomy, School of Medicine, Tokyo Women's Medical University, 162-8666, Japan, ††Department of Biological Sciences, Graduate School of Science, University of Tokyo, 113-8654, Japan, and ‡‡Program in Genetics and Epigenetics and §§Program in Biochemistry and Cell Biology, The University of Texas MD Anderson Cancer Center University of Texas Health Science Center Graduate School of Biomedical Sciences, Houston, Texas 77030

ORCID ID: 0000-0001-8261-6025 (M.E.C.)

ABSTRACT Studying genes involved in organogenesis is often difficult because many of these genes are also essential for early development. The allotetraploid frog, *Xenopus laevis*, is commonly used to study developmental processes, but because of the presence of two homeologs for many genes, it has been difficult to use as a genetic model. Few studies have successfully used CRISPR in amphibians, and currently there is no tissue-targeted knockout strategy described in *Xenopus*. The goal of this study is to determine whether CRISPR/Cas9-mediated gene knockout can be targeted to the *Xenopus* kidney without perturbing essential early gene function. We demonstrate that targeting CRISPR gene editing to the kidney and the eye of F0 embryos is feasible. Our study shows that knockout of both homeologs of *lhx1* results in the disruption of kidney development and function but does not lead to early developmental defects. Therefore, targeting of CRISPR to the kidney may not be necessary to bypass the early developmental defects reported upon disruption of Lhx1 protein expression or function by morpholinos, antisense RNA, or dominant negative constructs. We also establish a control for CRISPR in *Xenopus* by editing a gene (*slc45a2*) that when knocked out results in albinism without altering kidney development. This study establishes the feasibility of tissue-specific gene knockout in *Xenopus*, providing a cost-effective and efficient method for assessing the roles of genes implicated in developmental abnormalities that is amenable to high-throughput gene or drug screening techniques.

KEYWORDS CRISPR; kidney; targeted injection; *Xenopus laevis*; *lhx1*

XENOPUS laevis is a promising model for studying genes involved in human development and disease. *Xenopus* produce free-living, relatively transparent embryos, allowing for direct visualization of development and large-scale chemical screens (Tomlinson *et al.* 2005; Wheeler and Brändli 2009; Lienkamp *et al.* 2012). Large numbers of embryos are produced in a single clutch, allowing for hundreds of embryos to be manipulated by injection of antisense morpholino oligonucleotides or messenger RNAs (mRNAs). However, morpholino cost (~$400 each) and toxicity concerns have hindered the ability to conduct large-scale genetic screens. CRISPR gene editing has made the use of *Xenopus* to study organogenesis and human disease genes more feasible (Blitz *et al.* 2013; Nakayama *et al.* 2013; Guo *et al.* 2014; Bhattacharya *et al.* 2015; Naert *et al.* 2016, 2017; Banach *et al.* 2017). Established *Xenopus* fate maps enable targeted

doi: https://doi.org/10.1534/genetics.117.300468
Manuscript received September 28, 2017; accepted for publication November 18, 2017; published Early Online November 29, 2017.
Supplemental material is available online at www.genetics.org/lookup/suppl/doi:10.1534/genetics.117.300468/-/DC1.
[1]Present address: Department of Biological Sciences, Northern Arizona University, Flagstaff, AZ 86011.
[2]Corresponding author: University of Texas Health Science Center, 6431 Fannin St., MSE R414, Houston, TX 77030. E-mail: Rachel.K.Miller@uth.tmc.edu

microinjection into a selected blastomere that gives rise to an organ of interest (Moody 1987a,b; Moody and Kline 1990; Bauer *et al.* 1994; Karpinka *et al.* 2015; DeLay *et al.* 2016). Therefore, instead of generating conditional knockout mutant lines, *Xenopus* F0 embryos can be used to study gene function in a specific tissue, while avoiding early embryonic lethality associated with altering gene expression in the entire embryo.

Unlike mammalian metanephric kidneys, the *Xenopus* pronephros consists of a single functional nephron (Dressler 2006). The structure, as well as the spatial and developmental markers, is conserved between *Xenopus* pronephric and mammalian metanephric nephrons (Brändli 1999; Hensey *et al.* 2002). The *Xenopus* pronephros becomes functional within 2–3 days of fertilization, and visualization of the nephron through the epidermis makes *Xenopus* a simple model for studying genes affecting human kidney development and disease.

The LIM-class homeodomain transcription factor, *lhx1* (*lim1*), is essential for mouse placenta formation, and rare surviving *lhx1*-null mice lack head structures, kidneys, and reproductive organs (Shawlot and Behringer 1995; Kobayashi *et al.* 2005). In *Xenopus*, *lhx1* is expressed in the Spemann organizer and kidney (Taira *et al.* 1992, 1994). Injection of dominant negative *lhx1* constructs leads to anterior somite defects, bent body axis, and diminished pronephric development, and morpholino injection causes bent body axis (Chan *et al.* 2000; Kodjabachian *et al.* 2001; Hukriede *et al.* 2003; Rankin *et al.* 2011). Due to the essential role of *lhx1* in early development, targeted knockdown/out strategies have been employed to study its effects on mouse and *Xenopus* embryonic development. Therefore, *lhx1* was selected to test the feasibility of kidney-targeted CRISPR knockout.

This study is the first to examine tissue-targeted knockout strategies in *Xenopus*. We demonstrate that CRISPR knockout can be targeted to a tissue of interest in F0 *X. laevis* embryos and establish a control single guide RNA (sgRNA) against *slc45a2*, a gene necessary for pigment production in zebrafish and humans (Ko *et al.* 2012; Irion *et al.* 2014). We also show that *lhx1* knockout can be targeted to F0 embryonic kidneys, establishing the feasibility of using F0 *X. laevis* embryos for large-scale screens of genes implicated in human kidney disease. This targeting strategy can be easily applied to the study of other organ systems by selecting and injecting the appropriate blastomere in the early embryo (Moody 1987a,b; Moody and Kline 1990; Bauer *et al.* 1994; DeLay *et al.* 2016).

Materials and Methods

Embryos

Wild-type *X. laevis* adults were purchased from Nasco (LM00531MX) and embryos were obtained from these adults and reared as previously described (Sive *et al.* 2000). This protocol was approved by the University of Texas Health Science Center at Houston's Center for Laboratory Animal Medicine Animal Welfare Committee, which serves as the Institutional Animal Care and Use Committee (protocol #: AWC-16-0111).

sgRNA design and production

slc45a2 genomic sequence was obtained from Xenbase (http://xenbase.org) and *lhx1* sequences were obtained from the *X. laevis* genome browser at the Francis Crick Institute (http://genomes.crick.ac.uk/). sgRNAs against *slc45a2* and *lhx1* were designed using ZiFit (http://zifit.partners.org). Targets were blasted against the genome to ensure a unique hit and input into CRISPRscan to obtain predicted efficiency scores (http://www.crisprscan.org) (Moreno-Mateos *et al.* 2015). sgRNAs were designed to be complimentary to both the long and short chromosomes of *lhx1*. Slc45a2 transmembrane protein domains were determined and plotted using Protter (Omasits *et al.* 2014).

sgRNAs were produced using a PCR-based method (Bhattacharya *et al.* 2015). A modified universal reverse primer was used in conjunction with a gene-specific forward primer containing a T7 polymerase promoter (Table 1) to create a DNA template for subsequent sgRNA production (Bhattacharya *et al.* 2015).

T7 polymerase was purified from Rosetta cells transformed with RP-pETHis6-T7 RNA polymerase expression plasmid (Ellinger and Ehricht 1998). Two units of T7 polymerase were combined with 8 μl PCR product, 2 μl each of 75 mM dNTPs, and 2 μl 10X T7 buffer (40 mM Tris-HCl, 6 mM $MgCl_2$, 2 mM spermidine, 1 mM dithiothreitol, pH 7.9). The tube was incubated at 37° for 5 hr and 1 μl DNase was added, followed by a 15-min incubation at 37°. Fifteen microliters of ammonium acetate was added, and the reaction was brought up to 150 μl with RNase-free water. sgRNA was purified by acid phenol: chloroform extraction and ethanol precipitation.

Microinjection

Microinjections were performed as previously described (DeLay *et al.* 2016), with 10 nl of injection mix injected into individual blastomeres. For 8-cell injections, D1 blastomere was injected to target the eye, while the V2 blastomere was injected to target the kidney (Moody 1987a). sgRNA and Cas9 protein (CP01; PNA Bio) were incubated at room temperature for at least 5 min prior to co-injecting with either Alexa Fluor 488 fluorescent dextran or membrane-RFP RNA (Davidson *et al.* 2006; DeLay *et al.* 2016) tracers.

Genomic analysis

DNA was extracted from individual stage 10–12 embryos injected at the 1-cell stage (Bhattacharya *et al.* 2015). Regions surrounding the sgRNA target sites were amplified by PCR (Table 2). For *lhx1*, nested PCR was conducted to obtain the correct product. The *lhx1* outer primers were used for the first PCR reaction, followed by a second reaction using *lhx1* inner primers, with the resulting PCR product used for sequencing. PCR products were sequenced using the appropriate forward primer (Table 2). Insertion/deletion frequencies were calculated with TIDE (https://tide.nki.nl) (Brinkman *et al.* 2014).

Table 1 sgRNA production primers used in this study

Target gene	Sequence (5′ to 3′)	CRISPRscan score
Universal reverse	AAAAGCACCGACTCGGTGCCACTTTTTCAAGTTGATAACGGACTAGCCTTATTTTAACTTGCTATTTCTAGCTCTAAAAC	N/A
slc45a2	CTAGCTAATACGACTCACTATAGGTTACATAGGCTGCCTCCAGTTTTAGAGCTAGAAATAGCAAG	Unscored
lhx1 exon 1	CTAGCTAATACGACTCACTATAGGAGAAATGCTTCTCCAGGGGTTTTAGAGCTAGAAATAGCAAG	64
lhx1 exon 2	CTAGCTAATACGACTCACTATAGGTGTGCGGGCTGTGCCCAGGTTTTAGAGCTAGAAATAGCAAG	87
lhx1 exon 3	CTAGCTAATACGACTCACTATAGGCTCCCTTATGTGTCGGGTGTTTTAGAGCTAGAAATAGCAAG	58

Western blots

Embryos were staged (Nieuwkoop and Faber 1994) and collected to make protein lysates as previously described (Kim *et al.* 2002). One embryo equivalent of lysate was run in each well of an 8% SDS-PAGE gel. Protein was transblotted onto a 0.2-μm nitrocellulose membrane (GE Healthcare), and blocked for 3 hr (KPL block; SeraCare) at room temperature. Blots were incubated in 1:500 rabbit anti-Lhx1 primary antibody (Venegas-Ferrin *et al.* 2010) for 24 hr at 4° or 1:1000 rabbit anti-GAPDH (Santa Cruz FL-335) for 3 hr at room temperature. Blots were washed with TBST, incubated in goat anti-rabbit IgG horseradish peroxidase secondary antibody (1:5000; BioRad, Hercules, CA) for 2 hr at room temperature, and washed again with TBST prior to imaging (BioRad ChemiDoc XRS+) using enhanced chemiluminescence (Pierce Supersignal West Pico).

Immunostaining

Embryos were staged (Nieuwkoop and Faber 1994), fixed (DeLay *et al.* 2016), and immunostained using established protocols (Lyons *et al.* 2009). Proximal tubule lumens were labeled with 3G8 antibody (1:30) (Vize *et al.* 1995), and cell membranes of the intermediate, distal, and connecting tubules were labeled with 4A6 antibody (1:5) (Vize *et al.* 1995). Lhx1 was detected with Lhx1 antibody (1:250) (Venegas-Ferrin *et al.* 2010), and membrane-RFP tracer was labeled with RFP antibody (1:250; MBL International PM005). Goat anti-mouse IgG Alexa 488 (1:2000; Invitrogen, Carlsbad, CA), and goat anti-rabbit IgG Alexa 488 and Alexa 555 (1:2000; Invitrogen) secondary antibodies were used to visualize kidney and membrane-RFP tracer staining.

In situ hybridization

Digoxigenin-labeled RNA probes were prepared using a DIG RNA labeling kit (Roche). Constructs were linearized and synthesized using the listed enzyme and polymerase: *lhx1*-antisense *Xho*I/T7 (Taira *et al.* 1992; Carroll and Vize 1999), *hnf1β*-antisense *Sma*I/T7 (Demartis *et al.* 1994), *atp1a1*-antisense *Sma*I/T7b (Eid and Brändli 2001). Embryos were processed as described, eliminating the RNAse A/T1 step (Sive *et al.* 2000). 1:3000 dilution of Anti-DIG Fab fragments (Roche) and NBT/BCIP tablets (Roche) were used to detect probes.

Imaging

Embryos were scored and photographed using a Leica S8A80 stereomicroscope and Leica MC120 HD camera or an Olympus SZX16 fluorescent stereomicroscope and Olympus DP71 camera. 3G8/4A6 immunostained kidney images were taken using a Zeiss LSM800 confocal microscope. Images were processed with Adobe Photoshop and Illustrator CS6.

Data availability

Plasmids used in this study are available upon request. The authors declare that all data necessary for confirming the conclusions presented in the article are fully represented within the article.

Results

X. laevis CRISPR control

Knockout of *slc45a2* (chromosome 1L) results in eye and skin pigment loss, providing a phenotypic readout of CRISPR editing without affecting kidney development (Irion *et al.* 2014; Shigeta *et al.* 2016). Although *X. laevis* is allotetraploid, there is only one homeolog of the *slc45a2* gene: *slc45a2.L*. Therefore, the one sgRNA targeting the second exon of *slc45a2.L* (first transmembrane domain) hits the only copy of the gene (Figure 1A). Upon knockout, TIDE analysis indicated that *slc45a2* was edited mosaically in all five embryos tested (Supplemental Material, Figure S1) (Brinkman *et al.* 2014). Overall, 89.7% of the DNA was edited, resulting most commonly in a three-base deletion (Figure 1, B and C). Sequence decomposition near the sgRNA binding region (Figure 1D) was confirmed in all embryos examined (Figure S1). Although the most common mutation was a three-base deletion (Figure 1, E and F), individual embryos showed varying mutation profiles (Figure S1).

Since body pigment loss is difficult to assess, eye pigment loss was used to evaluate *slc45a2* gene editing efficiency (Figure 2A). Less than 50% loss was scored as "mild," >50% loss was scored as "moderate," and nearly complete loss was scored as "severe." Varying amounts of *slc45a2* sgRNA and Cas9 protein were injected into one cell of 2-cell embryos, and mortality and eye phenotype severity were assessed (Figure 2B). Of the conditions tested, 500 pg sgRNA and 1 ng Cas9 protein provided the best balance between phenotype severity and mortality (Figure 2B).

Tissue-targeted slc45a2 knockout

slc45a2 knockout was targeted to the eye by injecting embryos at the 1-, 2-, and 8-cell (left D1 blastomere) stages (Moody 1987a). Each of these injection stages showed eye

Table 2 Genotyping primers used in this study

Target gene	Forward sequence (5′ to 3′)	Reverse sequence (5′ to 3′)
slc45a2.L	GTTCCCTTCGCTCATACAATG[a]	GCCAGAAAGGGGTTTATTGC
lhx1.L exon 1 (outer primer set)	CCGTAGCACTGGACGTGATGT	CAGCTTAGGCTACCACACTGCCG[b]
lhx1.L exon 1 (inner primer set)	TGCCTTCTATTCTCCTAATCCGCCC[a,b]	GAAGAGTTTGCTCCTTGCCCTC
lhx1.S exon 1	CTGGACCGTTTCTTGTTGAATG[a]	GGTTTCACAAAGGGAAGTGCTG
lhx1.L exon 2	CAGCAAGAGATGTAGCCAGC[a]	GTCCTACAACTATGGCGAAACG
lhx1.S exon 2	CCTACAACAGTGGCGAAAC[a]	GTCCTCCATTCTTCCTACGG
lhx1.L exon 3	CATAGGGTGAAGAGGGCAAG[a]	CTCAAGTCTCCTTTGCAGCCAG
lhx1.S exon 3	CCATTTGCAAGTTGATACCC[a]	GGTGAGACGGTTCATAGTGTG

[a] Forward primer used for genomic sequencing.
[b] From Bachy *et al.* (2001).

pigment loss (Figure 2C). One-cell injections resulted in embryos with pigment loss in both eyes, while 2- and 8-cell injections caused pigment loss only on the injected side. Although embryos injected at the 2-cell stage exhibited both eye and trunk pigment loss, embryos properly injected at the 8-cell stage lost eye pigmentation but not pigmentation on the head or trunk (Figure 2C). Alexa 488:dextran tracer showed that 8-cell targeted injections yielded greater restriction to the eye than 1- or 2-cell injections. These data suggest that tissue-targeted knockout is possible and targeting *slc45a2* knockout to the eye produces embryos lacking eye pigmentation.

lhx1 knockout

lhx1 has two homeologs, located on chromosomes 2L and 2S. Three sgRNAs, each complimentary to both the long and short homeologs of *lhx1*, were designed to target exons 1, 2, and 3, corresponding to the first and second zinc finger and the homeobox domain of the Lhx1 protein, respectively (Figure 3A) (Table 1) (Sander *et al.* 2007, 2010; Moreno-Mateos *et al.* 2015). All three of the sgRNAs were designed so that there were no mismatches between the sgRNA target site and the sgRNA sequence on either of the *lhx1* homeologs.

Sequencing and TIDE analysis of DNA from stage 10–12 embryos indicates that the sgRNA targeting exon 1 was least efficient (Figure 3, B and D), resulting in mostly in-frame insertions (Figure 3, C and E), while editing of exon 2 was more efficient (Figure 3, F and H), resulting in mostly out-of-frame deletions and insertions (Figure 3, G and I). The sgRNA targeting exon 3 was most efficient, resulting in mostly a 5 bp out-of-frame deletion and a premature stop codon (Figure 3, J–M and Figure 4). The exon 3 sgRNA edited 64% of the DNA for both short and long homeologs (Figure 3, J and L). Additionally, the percent of aberrant sequences, defined as the difference in nucleotide chromatogram peak height between the unedited and knockout sequences, was significant downstream of the Cas9 cut site and greatly reduced upstream for the exon 3 sgRNA only (Figure S2). Individual embryos had similar editing efficiency of both the long and short homeologs (Figure 4), suggesting that the exon 3 sgRNA is able to efficiently edit both homeologs in the same embryo. Due to the greater editing efficiency of the exon 3 sgRNA, we chose to use this sgRNA for subsequent experiments.

lhx1 knockout disrupts pronephric development

lhx1 was knocked out at the 1-, 2-, or 8-cell stage (V2 blastomere) to target knockout to the kidney (Moody 1987a). As a negative control, *slc45a2* was knocked out. The kidney phenotype was rated as "mild" for slight impairments in kidney development, "moderate" if tubule regions were missing, and "severe" if kidney tubules were missing entirely. Kidneys were scored as "normal" if no differences existed between the injected and uninjected sides (Figure 5A). For embryos injected at the 1-cell stage, phenotype severity was assessed relative to *slc45a2* knockout embryos at the same stage.

Because *lhx1* knockout is embryonically lethal in mice, embryonic mortality was assessed upon targeting *lhx1* knockout to the kidney. We anticipated that 8-cell targeting would reduce embryo death compared to knockout in 1- or 2-cell embryos, but no difference in exogastrulation was observed for the three *lhx1* injection conditions ($P = 0.74$, Figure 5B).

The effect of *lhx1* knockout on kidney development was assessed in stage 39–41 embryos using antibodies to stain differentiated kidney tubules (3G8 and 4A6) (Vize *et al.* 1995). Embryos were injected at the 1-, 2-, or 8-cell (V2 blastomere) stages to assess the efficiency of kidney-targeted *lhx1* knockout. *lhx1* knockout disrupted proximal, distal, intermediate, and connecting tubule development for all three injection stages, while *slc45a2* knockout did not (Figure 5C). Embryos injected at the 2-cell stage exhibited the highest proportion of kidneys with moderate or severe phenotypes, while embryos injected at the 8-cell stage showed the lowest proportion of moderate or severe kidney phenotypes. Therefore, 2-cell injections were the most efficient at producing moderate and severe kidney phenotypic effects.

in situ staining with probes that label the majority of the pronephros (*hnf1β* and *atp1a1*) revealed decreased kidney tubulogenesis upon *lhx1* knockout (Figure 6A). Over 75% of the embryos injected at the 2- and 8-cell stages showed reduced *hnf1β* and *atp1a1* expression, with the majority displaying moderate or severe kidney phenotypes (Figure 6, C and D). In contrast, fewer embryos injected at the 1-cell stage showed moderate or severe phenotypes (Figure 6B), suggesting that 2- or 8-cell injections result in increased *lhx1* knockout phenotype severity in comparison to 1-cell injections.

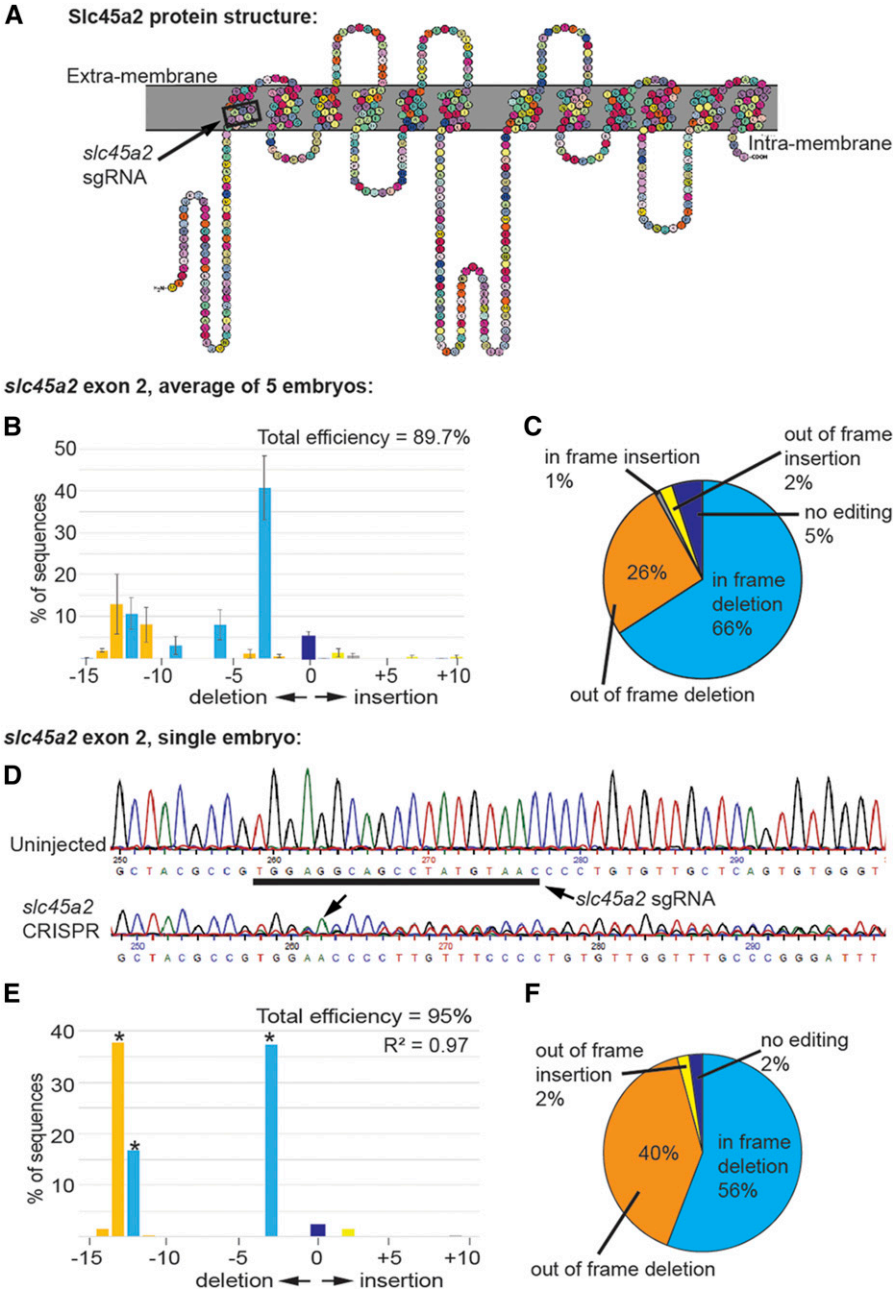

Figure 1 sgRNA targeting *slc45a2* efficiently edits *Xenopus* embryo DNA. All data shown are from stage 10–12 embryos injected with *slc45a2* sgRNA and Cas9 protein at the 1-cell stage. (A) Diagram of Slc45a2 protein showing the 12 transmembrane domains, with the region where the *slc45a2* sgRNA binds outlined in black. (B) Percent of sequenced *slc45a2* DNA containing different insertions and deletions. Bars shown are the mean of the percent of indel sequences from five individual embryos, error bars represent SEM. (C) Percent of indels that lead to in-frame or out-of-frame mutations. Data shown are the mean of the sequencing data from five individual embryos. (D–F) Results from a single representative embryo shown. (D) Sequencing chromatogram shows DNA editing after injection of *slc45a2* sgRNA and Cas9 protein. Underlined region indicates the sgRNA binding sequence. Arrow indicates the start of degradation of the sequence due to CRISPR editing. (E) TIDE analysis shows degradation of the sequence trace in the *slc45a2* CRISPR embryo after the expected Cas9 editing site. * $P < 0.001$ as identified by TIDE. (F) TIDE analysis prediction of the indels present in the single embryo, indicating that 3-, 12-, and 13-bp deletions are the most common indels in this embryo.

lhx1 knockout does not lead to head or axis defects

Because *lhx1* knockout did not lead to developmental head or axis defects seen using other techniques (Taira *et al.* 1992; Carroll and Vize 1999; Chan *et al.* 2000; Rankin *et al.* 2011), a *Xenopus* Lhx1 antibody was utilized to assess Lhx1 levels by immunoblot after CRISPR knockout (Venegas-Ferrin *et al.* 2010). Lhx1 levels were decreased in *lhx1* knockout embryos in comparison to *slc45a2* knockout embryos starting at stage 10–12 (Figure 7A and Figure S4), suggesting that *lhx1* knockout results in decreased Lhx1 protein production prior to axis establishment and kidney specification. Importantly, knockout did not result in complete loss of Lhx1, which may explain why the knockout embryos did not display head or axis defects.

Immunoblot analysis was performed to determine whether Lhx1 protein was present prior to zygotic transcription initiation. Lhx1 protein was first detected in 1-cell embryos, with increased expression around gastrulation (stage 10–12) after the midblastula transition (Figure 7B). Lhx1 levels decreased between stages 25 and 30 and increased during later tadpole stages (35–40), corresponding to previously published mRNA expression data (Taira *et al.* 1992; Session *et al.* 2016; Watanabe *et al.* 2017) and the results seen in *slc45a2* knockout embryos (Figure 7A). Taken together, these data indicate that low levels of maternally loaded *lhx1* RNA and/or Lhx1 protein may compensate for the genomic knockout during head formation, and that knockout of *slc45a2* does not alter the embryo stage-specific Lhx1 expression pattern.

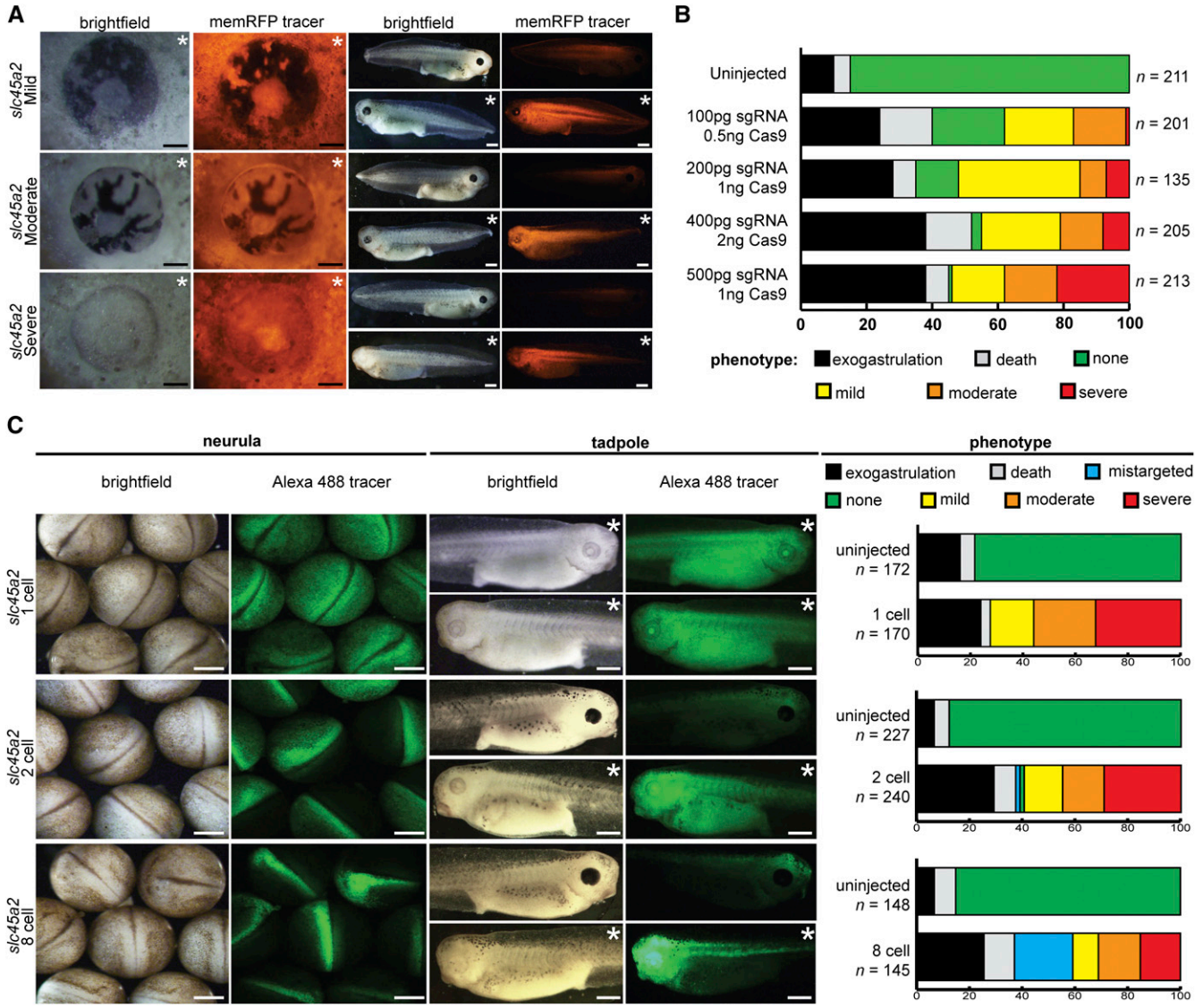

Figure 2 *slc45a2* knockout results in loss of eye and body pigmentation and can efficiently be targeted to the eye. (A) Phenotype severity scoring system based on pigment loss in the eye. Mild phenotype: >50% of eye pigment present; moderate phenotype: <50% of eye pigment present; severe phenotype: almost no eye pigment present. Embryos injected with 500 pg *slc45a2* sgRNA, 1 ng Cas9 protein, and memRFP RNA tracer in one cell of a 2-cell embryo. (B) Survival and phenotype severity of embryos injected with varying amounts of *slc45a2* sgRNA and Cas9 protein. Exogastrulation: embryo death prior to gastrulation; death: embryo death after gastrulation and before stage 39–41; none: no eye pigment loss. Surviving stage 39–41 embryos were scored based on phenotype severity. (C) Phenotype severity eye-targeted CRISPR gene editing. Embryos injected with 500 pg *slc45a2* sgRNA, 1 ng Cas9 protein, and Alexa 488 dextran tracer at 1-, 2-, and 8-cell stages (blastomere D1) show *slc45a2* editing in the targeted eye tissue. Embryos shown at neurula (NF stage 19–20) and tadpole (NF stage 39–41) stages. Mistargeted: tracer not present in the eye. (A and C) White bar, 500 μm, black bar, 100 μm. * Injected side of embryo.

in situ analysis of stage 20 embryos was conducted to determine whether knockout affects early kidney development. *lhx1* knockout in 2-cell embryos resulted in decreased *lhx1* expression in the kidney anlagen, indicating a loss of *lhx1* transcript (Figure 7C). No decrease in *lhx1* staining in the neural structures was observed in the *lhx1* knockout embryos (Figure 7C).

To confirm that knockout decreases Lhx1 protein levels within the kidney, embryos were injected in one cell at the 2-cell stage and immunostained at stage 30 using an Lhx1 antibody that stains the nucleus of kidney cells and neural structures (Irion *et al.* 2014). *Lhx1* knockout embryos showed reduced Lhx1 in the kidney on the injected side in comparison to the uninjected side of the embryo (Figure 7D). Similar to the range of kidney loss seen in later stage embryos visualized with 3G8 and 4A6 antibodies, we observed a range of *lhx1* expression loss in *lhx1* knockout embryos (Figure S3).

Knockout of lhx1 leads to edema

Assessment of edema was used as a readout of kidney function. Injections into both cells of 2-cell embryos resulted in

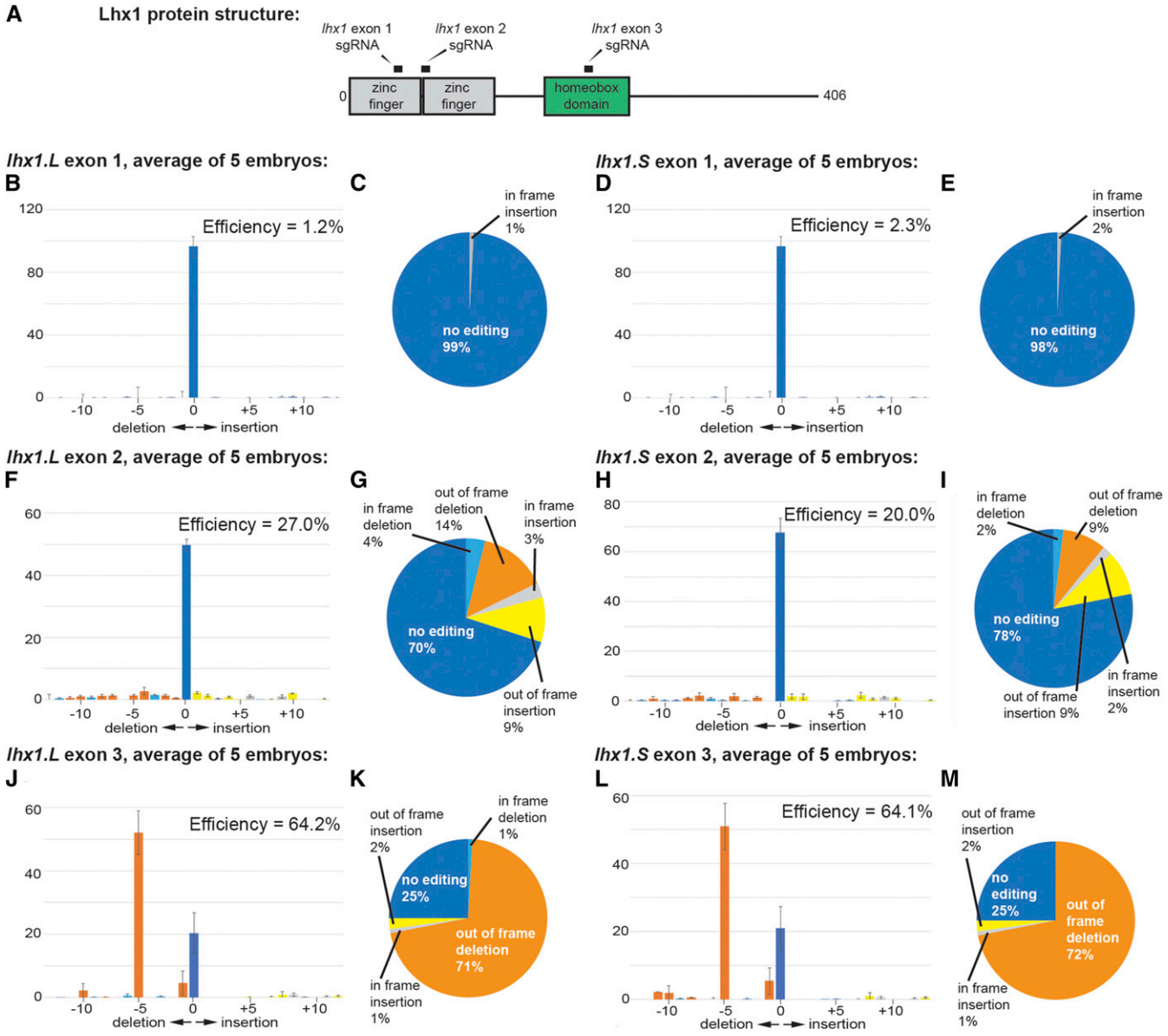

Figure 3 Comparison of the editing efficiency of three different sgRNAs designed to edit *lhx1*. (A) Diagram of the domains present in Lhx1 protein. Regions corresponding to the three *lhx1* sgRNAs used in this study are represented by the black bars above the protein domains. Each sgRNA was complementary to both *lhx1.L* and *lhx1*.S. (B, C, F, G, J, and K) TIDE analysis results from the long chromosome, with pooled results from five embryos reported. (D, E, H, I, L, and M) TIDE analysis results from the short chromosome, with pooled results from five embryos reported. (B, D, F, H, J, and L) Percentage of DNA editing contributed to insertions and deletions of different sizes. Error bars represent the SEM. (C, E, G, I, K, and M) Percent of in-frame and out-of-frame insertions and deletions.

edema in the head and thorax (Figure 8A) (Nieuwkoop and Faber 1994). Sixty percent of *lhx1* knockout embryos displayed edema, compared to 3% of *slc45a2* knockout controls (Figure 8B). Prior to edema development (stage 43–46), the embryos looked phenotypically normal and did not display head or axis defects.

Immunostaining showed that none of the *lhx1* knockout embryos displaying edema had normal kidneys (Figure 8C), while all of the *lhx1* knockout embryos without edema had at least one normal kidney. Likewise, the majority of the *slc45a2* knockout embryos had two normal kidneys. These data suggest that *lhx1* knockout prevents functional kidney formation.

Discussion

CRISPR gene editing is new in the allotetraploid *X. laevis* (Lane *et al.* 2015; Wang *et al.* 2015; Jaffe *et al.* 2016; Banach *et al.* 2017), and tissue-targeted CRISPR knockouts have not been reported. Our results indicate that CRISPR can efficiently target a tissue of interest. Although *X. laevis* has two homeologs for many of its genes, our results demonstrate

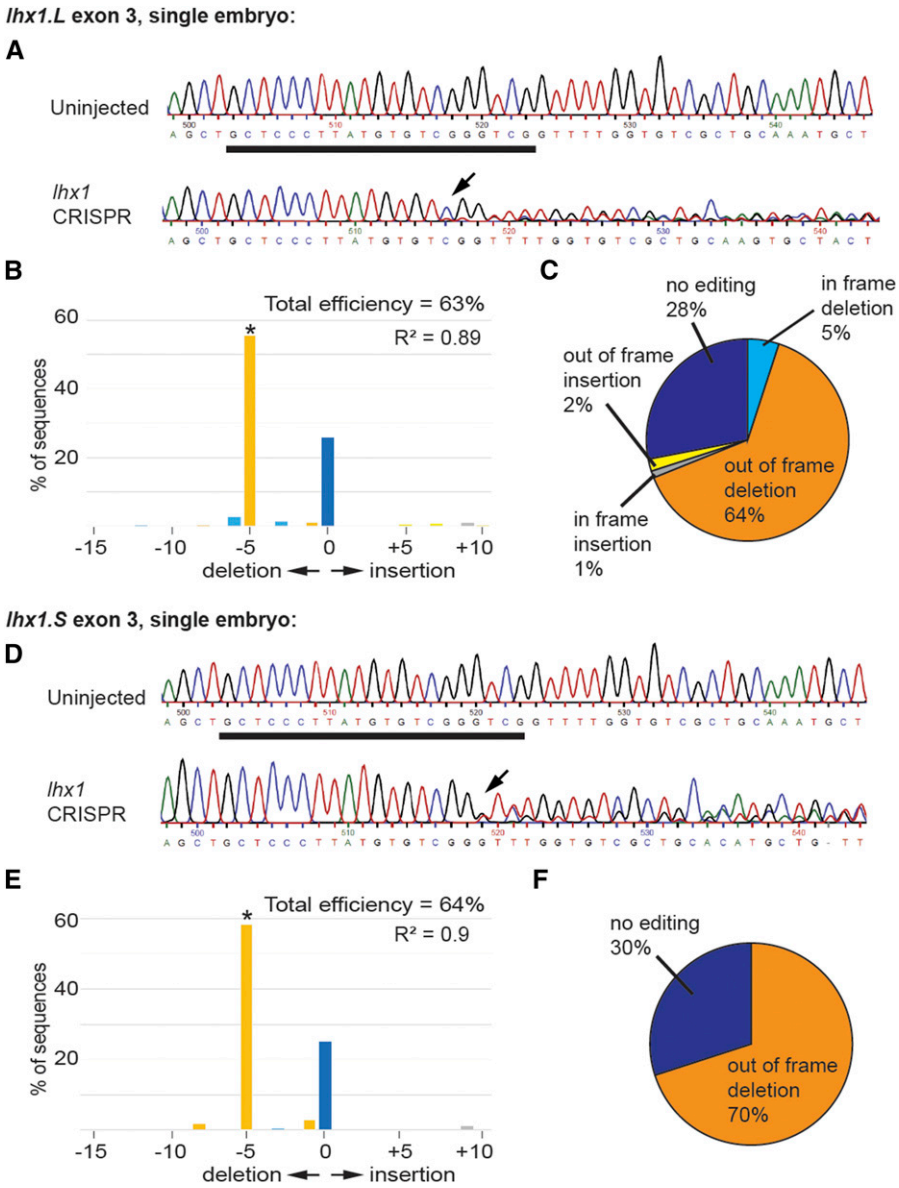

Figure 4 Comparison of the editing efficiency of *lhx1* exon 3 sgRNA in a single embryo. Results shown in A–C and D–F are from the same embryo. (A–C) Editing efficiency in *lhx1.L*. (D–F) Editing efficiency in *lhx1.S*. (A and D) Sequencing chromatogram showing degradation of the sequence in the region of the sgRNA binding site. Underlined region corresponds to the sgRNA binding site, and the black arrow marks the point of sequence degradation in the *lhx1* knockout embryo. (B and E) TIDE analysis results from a single embryo showing percentage of DNA editing due to insertions and deletions of different sizes. * $P < 0.001$ as identified by TIDE. (C and F) Percent of in-frame and out-of-frame insertions and deletions.

that a single sgRNA can efficiently target both homeologs in F0 embryos. In fact, the sgRNA tested gave similar DNA editing efficiencies for both homeologs of *lhx1*.

We observed a range of pigment loss phenotypes upon knockout of *slc45a2* ranging from mild to complete pigment loss. Approximately 40% of the total DNA sequenced from five individual embryos had a 3-bp deletion, while ~26% had an out-of-frame deletion. Each embryo is mosaic, with individual cells (and alleles within those cells) potentially having different *slc45a2* mutations. This was evidenced by our sequencing results, which showed that individual embryos displayed a range of mutations (Figure 1, D–F). It is unlikely that the in-frame deletions had no effect on *slc45a2* function, as these mutations account for the vast majority of the sequenced mutations, and the majority of the surviving embryos were missing more than half the pigment in their eye (moderate and severe phenotypes). Instead, it is possible that the variation in pigmentation that was observed in our *slc45a2* knockout embryos is due to functional maternal RNA or protein, or incomplete penetrance. We used wild-type, pigmented *Xenopus* for this study. The adult frogs and resulting embryos display varying degrees of pigmentation. Therefore, if the parent is highly pigmented, this may have an effect on the embryo's pigment as well. In fact, *slc45a2* mRNA levels are highest in unfertilized oocytes, suggesting that maternal effects may play a role in an embryo's pigmentation (Session *et al.* 2016).

lhx1 knockout led to abnormally developed kidney tubules in embryos injected at the 1-, 2-, and 8-cell stages. Injecting embryos at the 2-cell stage results in embryos with one *lhx1* knockout kidney and one unedited kidney, serving as an internal control. No advantage to targeting at the 8-cell stage in comparison to injecting one cell of a 2-cell embryo was observed. Eight-cell microinjections are challenging because

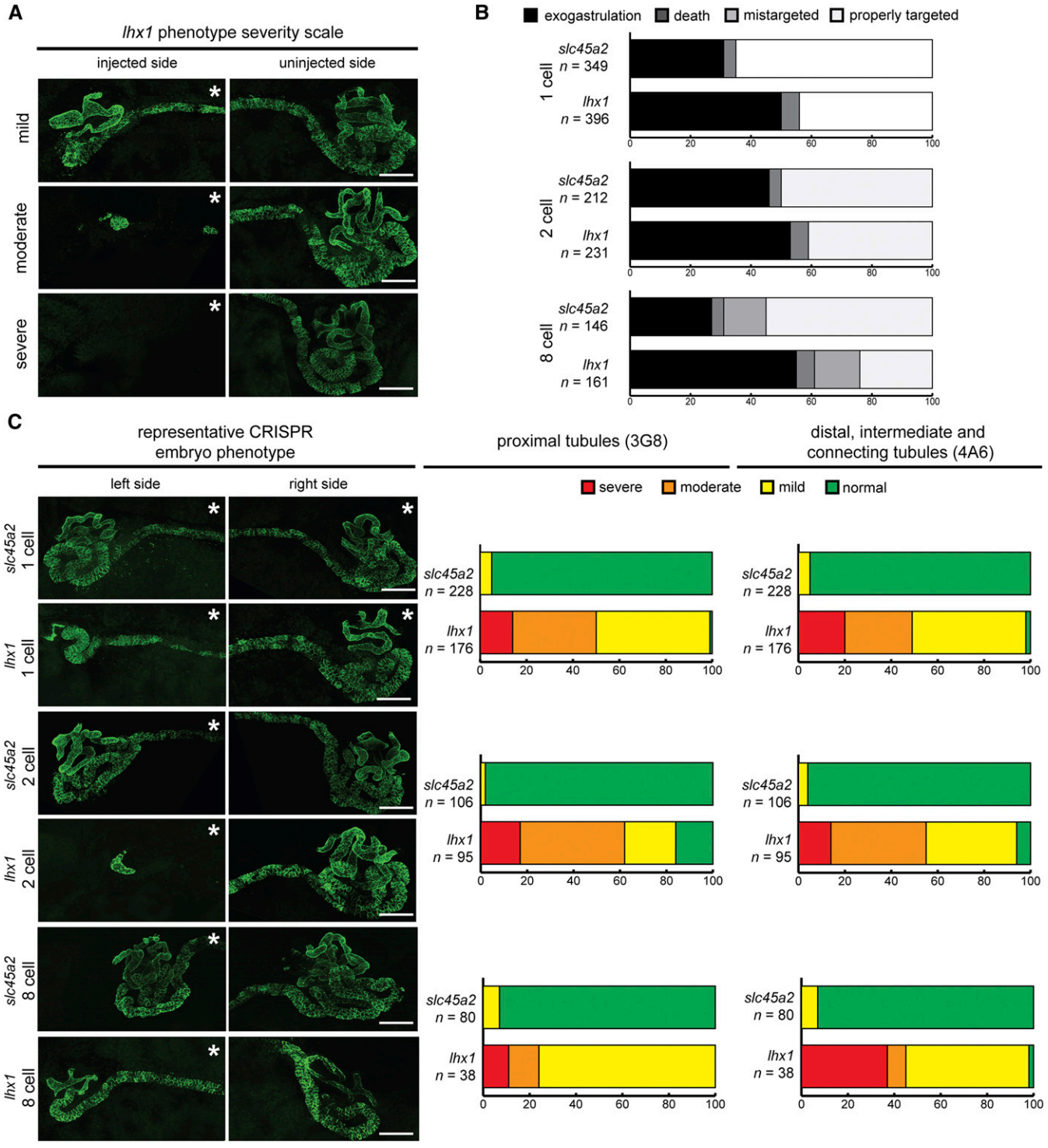

Figure 5 Knockout of *lhx1* leads to kidney developmental defects. (A) Scoring system used to assess the phenotypic severity of *lhx1* knockout embryos. Mild: decrease in kidney tubulogenesis in comparison to the uninjected side of the embryo; moderate: portions of the kidney tubules missing; severe: kidney tubules absent. Embryos stained with antibodies 3G8 (to label proximal tubule lumen) and 4A6 (to label the cell membranes of the intermediate, distal, and connecting tubules). (B) Targeting CRISPR knockout of *lhx1* to the kidney does not decrease embryo mortality. Embryos injected at the 1-, 2- and 8-cell (blastomere V2) stages. Exogastrulation: embryos die during gastrulation; death: embryos survive gastrulation but die prior to stage 40; mistargeted: tracer not present in the kidney. (C) *lhx1* targeted knockout reduces late markers of kidney development. Embryos assessed at stage 39–41 using immunostaining with 3G8 and 4A6 antibodies. (A and C) * denotes injected side of embryo. White bar, 100 μm.

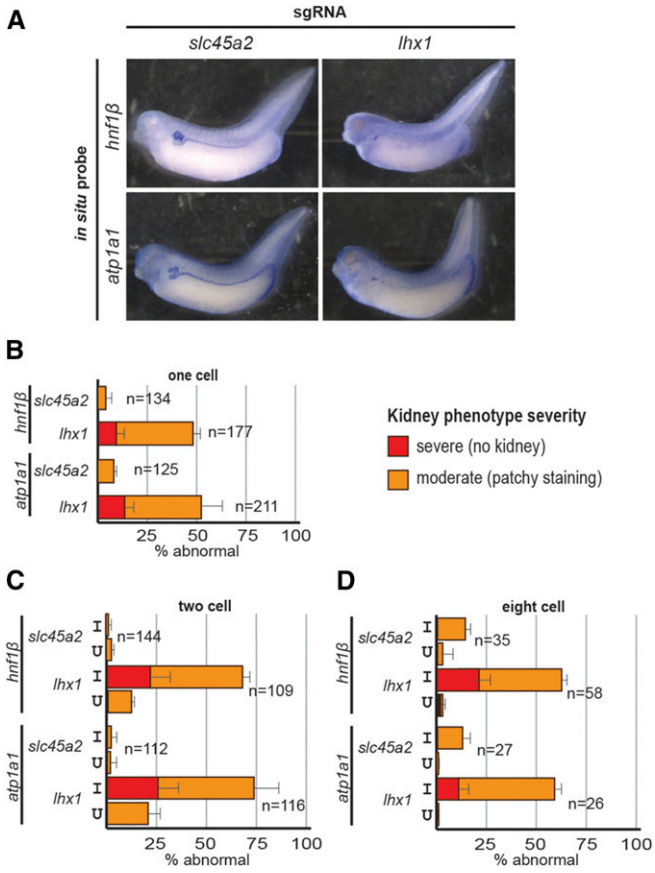

Figure 6 Knockout of *lhx1* leads to a decrease in kidney developmental markers as seen by *in situ* hybridization. (A) Representative embryos showing that knockout of *lhx1* leads to a decrease in *hnf1β* and *atp1a1* expression in the pronephros, while *slc45a2* knockout does not cause a decrease in these markers of kidney development. (B) *lhx1* knockout in 1-cell embryos leads to a decrease in *hnf1β* and *atp1a1* in comparison to *slc45a2* knockout control embryos. (C) *lhx1* knockout in 2-cell embryos leads to a decrease in *hnf1β* and *atp1a1* in comparison to *slc45a2* knockout control embryos. (D) *lhx1* knockout in 8-cell embryos leads to a decrease in *hnf1β* and *atp1a1* in comparison to *slc45a2* knockout control embryos. I, injected side of embryo; U, uninjected side of embryo.

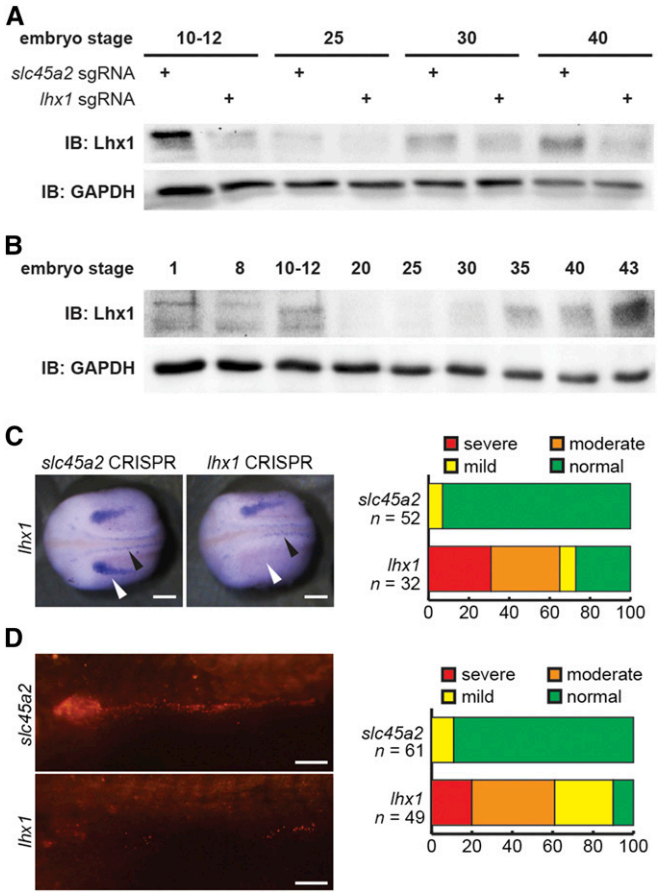

Figure 7 Lhx1 protein and *lhx1* RNA levels are decreased upon CRISPR knockout. (A) Immunoblot (IB) showing that knockout of *lhx1* leads to a decrease in Lhx1 protein in comparison to *slc45a2* knockout controls as early as embryonic stage 10–12. One-cell embryos were injected with 1 ng Cas9 protein and 500 pg of either *slc45a2* or *lhx1* sgRNA. (B) Immunoblot of embryo lysates from different stages of *Xenopus* development, ranging from 1-cell embryo (stage 1) to tadpole (stage 43). Levels of Lhx1 and GAPDH (loading control) protein show that Lhx1 is present in embryos throughout pronephric development (stages 12.5–43). (C) *lhx1 in situ* of stage 20 embryos shows loss of kidney staining on the injected side (white arrowheads) of *lhx1* CRISPR embryos, but not in *slc45a2* CRISPR embryos. No decrease in neural staining in the *lhx1* knockout embryos was observed in comparison to the *slc45a2* controls (black arrowheads). CRISPR knockout done in one cell of 2-cell embryos. White bar, 200 μm. Graph depicts severity of *lhx1* loss on the injected side of the embryo. None: no loss of *lhx1* staining; mild: decrease in *lhx1* staining; moderate: patchy loss of *lhx1* staining; severe: complete loss of *lhx1* staining. (D) *lhx1* immunostaining of stage 32 embryos shows loss of kidney staining on the injected side of *lhx1* CRISPR embryos, but not in *slc45a2* CRISPR embryos. CRISPR knockout done in one cell of 2-cell embryos. The epidermis of the embryo was removed prior to imaging. White bar, 100 μm. Graph depicts severity of *lhx1* immunostaining loss on the injected side of the embryo. None: no loss of *lhx1* staining; mild: decrease in *lhx1* staining; moderate: patchy loss of *lhx1* staining; severe: complete loss of *lhx1* staining.

the embryo must be turned prior to injection, and identification of the correct cell can be difficult, while at the 2-cell stage either blastomere can be injected. As early developmental defects are not seen with 2-cell injections, CRISPR editing of genes implicated in kidney development can be carried out at the 2-cell stage, which is not a viable strategy for morpholino-mediated knockdown of essential genes.

Of the three *lhx1* sgRNAs tested, the sgRNA targeting exon 3 was most efficient, although its predicted efficiency was the least (Table 1). Additionally, the *slc45a2* sgRNA resulted in editing of over 89% of the DNA, but CRISPRscan did not score this sgRNA. Although CRISPRscan was designed against a library of *Xenopus tropicalis* sgRNAs, our results suggest that guide quality predicted by this software does not necessarily apply to *X. laevis*.

lhx1 plays an important role in early embryonic development of head structures in both mice and *Xenopus* (Shawlot and Behringer 1995; Yasuoka *et al.* 2014). In mouse, *lhx1* knockout is embryonically lethal (Shawlot and Behringer 1995). For this reason, previous *lhx1* loss-of-function studies in *Xenopus* were accomplished by targeted injection to bypass early developmental defects (Chan *et al.* 2000; Hukriede

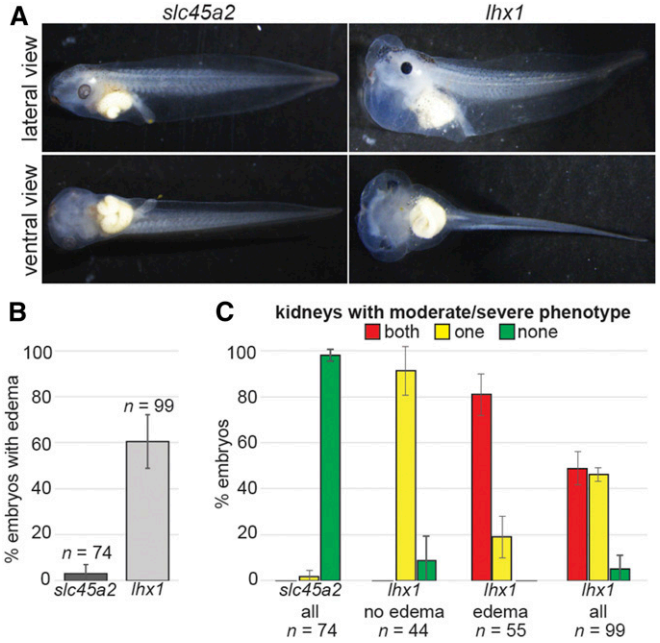

Figure 8 Knockout of *lhx1* leads to edema formation. Embryos were injected into both cells of 2-cell embryos with 1 ng Cas9 protein and 500 pg of either *slc45a2* or *lhx1* sgRNA, and reared to stage 43–46 for immunostaining and scoring. Error bars represent the SEM. (A) Knockout of *lhx1* leads to edema formation in *Xenopus* embryos. (B) The percent of *lhx1* knockout embryos displaying edema at stage 43–46 is higher than *slc45a2* control embryos. (C) Percent of embryos with moderate (missing parts) and severe (absent) kidney phenotypes. Most *lhx1* knockout embryos with edema display moderate/severe kidney phenotypes in both kidneys, while most embryos without edema have at least one normal kidney.

et al. 2003; Cirio *et al.* 2011; Rankin *et al.* 2011). Unexpectedly, we found no difference in lethality between embryos injected at the 1-, 2-, or 8-cell stages. We did not observe early developmental defects (missing head structures, bent spines) in *lhx1* knockout embryos, suggesting that targeted knockout is not necessary. However, disrupted kidney development was observed as reported in prior knockdown studies (Chan *et al.* 2000; Cirio *et al.* 2011). Similar to mouse, we found that *lhx1* knockout led to kidneys with regions of the tubules missing, suggesting that there are multiple points of kidney induction (Kobayashi *et al.* 2005).

Although the majority of *lhx1* knockout embryos displayed kidney defects, we did not observe head or axis defects. There are multiple potential explanations for this observation. Unlike morpholinos or dominant negative constructs, CRISPR should not affect maternal protein or RNA (Watanabe *et al.* 2017). Prior studies suggest that CRISPR may not influence early *Xenopus* embryonic development due to unaffected maternal mRNA and protein deposits (Bhattacharya *et al.* 2015). Alternatively, the low levels of Lhx1 protein in knockout animals may be enough for the head organizer to develop normally, whereas pronephric development may be more sensitive to lower Lhx1 levels. The mosaic nature of *lhx1* knockout may allow the embryos to develop without early developmental defects, because unlike the organizer, the pronephros may be affected cell-autonomously by *lhx1* knockout. Similar to our results, morpholino knock down of β-catenin in *X. tropicalis* results in ventralization, but CRISPR knockout does not (Bhattacharya *et al.* 2015). These data suggest that CRISPR knockout in F0 embryos of *Xenopus* and other models, such as zebrafish, may be useful to study genes that are embryonically lethal in null mutants, especially for studying later developmental processes such as organ formation. To disrupt early developmental processes, such as dorsal organizer function, it may be necessary to perform "leap-frogging" to knock out the gene only in the germ cells or oocyte transfer to create F0 mutations (Blitz *et al.* 2016; Aslan *et al.* 2017).

Successful knockout of *lhx1* in F0 embryos requires editing of all four *lhx1* alleles to produce a complete loss-of-function phenotype. Additionally, all four alleles must be edited in a way that produces a non-functional protein, such as with out-of-frame insertions or deletions. The *lhx1*-knockout embryos produced in this study showed a range of phenotypes, from a decrease in tubule development to a complete loss of tubules. One possible explanation for the range of observed phenotypes is that embryos with the most severe phenotype have all four *lhx1* alleles edited, while embryos with moderate and mild phenotypes have one or more unedited *lhx1* alleles. Sequencing of the two *lhx1* homeologs showed that ~64% of the *lhx1.L* and *lhx1.S* DNA was edited. Therefore, the probability that all four alleles were edited in a single cell was ~41%. This frequency is similar to the range of phenotypes observed in knockout embryos, with the phenotype severity likely corresponding to the percentage of cells that have all four alleles knocked out. Therefore, it is possible that embryos with a severe phenotype have all four alleles edited in most of their kidney cells, while embryos that have a moderate or mild phenotype have one or more unedited *lhx1* alleles in the majority of their kidney cells.

The two genes knocked out in this study, *slc45a2* and *lhx1*, have known functions in human, mouse, and *Xenopus* (Shawlot and Behringer 1995; Chan *et al.* 2000; Kodjabachian *et al.* 2001; Hukriede *et al.* 2003; Kobayashi *et al.* 2005; Rankin *et al.* 2011; Ko *et al.* 2012). Although the F0 embryos generated in this study displayed varying phenotype severities, the resulting pigment loss and kidney defect phenotypes were as expected from previous *X. tropicalis* and *Danio rerio* CRISPR knockout (*slc45a2*) and *X. laevis* knockdown (*lhx1*) studies (Cirio *et al.* 2011; Irion *et al.* 2014; Shigeta *et al.* 2016). We saw a range of phenotype severities in the *slc45a2* and *lhx1* knockout embryos, similar to what has been reported in other reports of *slc45a2* CRISPR knockout in *X. tropicalis* and antisense knockdown of *lhx1* (Cirio *et al.* 2011; Shigeta *et al.* 2016). Therefore, our results show that CRISPR is a reliable way of producing large numbers of F0 embryos with known genetic knockout phenotypes. However, the range of phenotypes observed in our knockout embryos may make the characterization of the function of unknown genes more difficult. In this case, CRISPR may be a good option for quickly and

cheaply screening large numbers of genes for potential phenotypic effects. When a gene is found to produce a phenotype in F0 embryos, follow-up experiments can be performed to verify gene function. Alternatively, mutant lines may be bred to create homozygous F1 individuals with known genetic mutations. Although it may be easy to create lines with knockout of nonessential genes like *slc45a2*, a knockout line with a gene such as *lhx1* may not be feasible. In this case, phenotypic analysis of F0 embryos may be a more effective strategy for studying the function of essential genes.

X. laevis is a unique model for studying genes implicated in human diseases using CRISPR genome editing (Tandon *et al.* 2017). Approximately 79% of genes implicated in human diseases have *Xenopus* orthologs, including genes that are involved in human kidney disorders (Hellsten *et al.* 2010). In addition, *Xenopus* embryos develop functional kidneys within 2–3 days of fertilization, allowing for the assessment of large numbers of F0 mutant kidneys in a short time. Therefore, CRISPR genome editing allows for high-throughput screening of candidate human disease genes with the benefit that each embryo has an uninjected control side. Although we showed that targeted CRISPR knockout is highly efficient in the eye and kidney, the technique described here would be applicable to the study of other organs in the developing *Xenopus* embryo. The quick embryonic development time, large clutch size, and ability to target a tissue of interest on one side of the embryo make CRISPR genome editing in *X. laevis* an innovative model for the study of human gene function and genetic disorders.

Acknowledgments

We thank the instructors and teaching assistants of the 2015 and 2016 Cold Spring Harbor Laboratory *Xenopus* Course, in particular K.J. Liu, M.K. Khokha, and E.K. Mis, for training in *Xenopus* CRISPR gene editing and *in situ* hybridization techniques. The instructors of the 2017 National *Xenopus* Resource *Xenopus* Genome Editing Workshop also provided advice on genome editing techniques. We also thank N.R. De Lay for the gift of the T7 polymerase expression plasmid and Rosetta cells, as well as for advice on sgRNA production and purification. We are grateful to the members of the laboratories of R.K.M. and P.D. McCrea, as well as to M. Kloc, for their helpful suggestions and advice throughout this project. In particular, we thank V. Krneta-Stankic for early help with injections. Additionally, we thank S.-T. Yen for assessing the *lhx1* CRISPR sgRNA sequences, as well as S. McNamara and N. Aryal for guidance on CRISPR sgRNA design. We especially thank R.R. Behringer for advice on CRISPR knockout of *lhx1* and for critically reading this article and providing guidance throughout this project. We are grateful to the University of Texas Health Science Center Office of the Executive Vice President and Chief Academic Officer and the Department of Pediatrics Microscopy Core for funding and maintaining the Zeiss LSM800 confocal microscope used in this work. These studies were supported by a National Institutes of Health (NIH) KO1 grant (K01DK092320 to R.K.M.), startup funding from the Department of Pediatrics Pediatric Research Center at the University of Texas McGovern Medical School (to R.K.M.), an NIH National *Xenopus* Resource Center grant (P40OD010997 to M.E.H.), and an NIH R01 grant (R01HD084409 to M.E.H.).

Author contributions: B.D.D. performed microinjections, sequencing and TIDE analysis, analyzed embryo phenotypes, and wrote the article. M.E.C. performed microinjections, *in situ* hybridization, and edema experiments. H.L.H. performed microinjections. M.S. and M.E.H. designed the *slc45a2* sgRNA. J.M.D. helped to design and generate the *lhx1* sgRNAs. N.S. and M.T. generated the Lhx1 antibody. R.K.M. conceived of the project, helped to design the *lhx1* sgRNAs, and oversaw the experiments and article preparation. All authors critically read and edited the article.

Literature Cited

Aslan, Y., E. Tadjuidje, A. M. Zorn, and S. W. Cha, 2017 High-efficiency non-mosaic CRISPR-mediated knock-in and indel mutation in F0 *Xenopus*. Development 144: 2852–2858.

Bachy, I., P. Vernier, and S. Retaux, 2001 The LIM-homeodomain gene family in the developing *Xenopus* brain: conservation and divergences with the mouse related to the evolution of the forebrain. J. Neurosci. 21: 7620–7629.

Banach, M., E. S. Edholm, and J. Robert, 2017 Exploring the functions of nonclassical MHC class Ib genes in *Xenopus laevis* by the CRISPR/Cas9 system. Dev. Biol. 426: 261–269.

Bauer, D. V., S. Huang, and S. A. Moody, 1994 The cleavage stage origin of Spemann's organizer: analysis of the movements of blastomere clones before and during gastrulation in *Xenopus*. Development 120: 1179–1189.

Bhattacharya, D., C. A. Marfo, D. Li, M. Lane, and M. K. Khokha, 2015 CRISPR/Cas9: an inexpensive, efficient loss of function tool to screen human disease genes in *Xenopus*. Dev. Biol. 408: 196–204.

Blitz, I. L., J. Biesinger, X. Xie, and K. W. Cho, 2013 Biallelic genome modification in F0 *Xenopus tropicalis* embryos using the CRISPR/Cas system. Genesis 51: 827–834.

Blitz, I. L., M. B. Fish, and K. W. Cho, 2016 Leapfrogging: primordial germ cell transplantation permits recovery of CRISPR/Cas9-induced mutations in essential genes. Development 143: 2868–2875.

Brändli, A. W., 1999 Towards a molecular anatomy of the *Xenopus* pronephric kidney. Int. J. Dev. Biol. 43: 381–395.

Brinkman, E. K., T. Chen, M. Amendola, and B. van Steensel, 2014 Easy quantitative assessment of genome editing by sequence trace decomposition. Nucleic Acids Res. 42: e168.

Carroll, T., and P. D. Vize, 1999 Synergism between Pax-8 and lim-1 in embryonic kidney development. Dev. Biol. 214: 46–59.

Chan, T. C., S. Takahashi, and M. Asashima, 2000 A role for Xlim-1 in pronephros development in *Xenopus laevis*. Dev. Biol. 228: 256–269.

Cirio, M. C., Z. Hui, C. E. Haldin, C. C. Cosentino, C. Stuckenholz *et al.*, 2011 Lhx1 is required for specification of the renal progenitor cell field. PLoS One 6: e18858.

Davidson, L. A., M. Marsden, R. Keller, and D. W. Desimone, 2006 Integrin alpha5beta1 and fibronectin regulate polarized cell protrusions required for *Xenopus* convergence and extension. Curr. Biol. 16: 833–844.

DeLay, B. D., V. Krneta-Stankic, and R. K. Miller, 2016 Technique to target microinjection to the developing *Xenopus* kidney. J. Vis. Exp. 111: 10.3791/53799.

Demartis, A., M. Maffei, R. Vignali, and G. Barsacchi, 1994 Cloning and developmental expression of LFB3/HNFIβ transcription factor in *Xenopus laevis*. Mech. Dev. 47: 19–28.

Dressler, G. R., 2006 The cellular basis of kidney development. Annu. Rev. Cell Dev. Biol. 22: 509–529.

Eid, S. R., and A. W. Brändli, 2001 *Xenopus* Na,K-ATPase: primary sequence of the beta2 subunit and in situ localization of alpha1, beta1, and gamma expression during pronephric kidney development. Differentiation 68: 115–125.

Ellinger, T., and R. Ehricht, 1998 Single-step purification of T7 RNA polymerase with a 6-histidine tag. Biotechniques 24: 718–720.

Guo, X., T. Zhang, Z. Hu, Y. Zhang, Z. Shi *et al.*, 2014 Efficient RNA/Cas9-mediated genome editing in *Xenopus tropicalis*. Development 141: 707–714.

Hellsten, U., R. M. Harland, M. J. Gilchrist, D. Hendrix, J. Jurka *et al.*, 2010 The genome of the Western clawed frog *Xenopus tropicalis*. Science 328: 633–636.

Hensey, C., V. Dolan, and H. R. Brady, 2002 The *Xenopus* pronephros as a model system for the study of kidney development and pathophysiology. Nephrol. Dial. Transplant. 17: 73–74.

Hukriede, N. A., T. E. Tsang, R. Habas, P. L. Khoo, K. Steiner *et al.*, 2003 Conserved requirement of Lim1 function for cell movements during gastrulation. Dev. Cell 4: 83–94.

Irion, U., J. Krauss, and C. Nüsslein-Volhard, 2014 Precise and efficient genome editing in zebrafish using the CRISPR/Cas9 system. Development 141: 4827–4830.

Jaffe, K. M., D. T. Grimes, J. Schottenfeld-Roames, M. E. Werner, T. S. Ku *et al.*, 2016 c21orf59/kurly controls both cilia motility and polarization. Cell Rep. 14: 1841–1849.

Karpinka, J. B., J. D. Fortriede, K. A. Burns, C. James-Zorn, V. G. Ponferrada *et al.*, 2015 Xenbase, the *Xenopus* model organism database; new virtualized system, data types and genomes. Nucleic Acids Res. 43: D756–D763.

Kim, S. W., X. Fang, H. Ji, A. F. Paulson, J. M. Daniel *et al.*, 2002 Isolation and characterization of XKaiso, a transcriptional repressor that associates with the catenin Xp120(ctn) in *Xenopus laevis*. J. Biol. Chem. 277: 8202–8208.

Ko, J. M., J. A. Yang, S. Y. Jeong, and H. J. Kim, 2012 Mutation spectrum of the TYR and SLC45A2 genes in patients with oculocutaneous albinism. Mol. Med. Rep. 5: 943–948.

Kobayashi, A., K. M. Kwan, T. J. Carroll, A. P. McMahon, C. L. Mendelsohn *et al.*, 2005 Distinct and sequential tissue-specific activities of the LIM-class homeobox gene Lim1 for tubular morphogenesis during kidney development. Development 132: 2809–2823.

Kodjabachian, L., A. A. Karavanov, H. Hikasa, N. A. Hukriede, T. Aoki *et al.*, 2001 A study of Xlim1 function in the Spemann-Mangold organizer. Int. J. Dev. Biol. 45: 209–218.

Lane, A. B., M. Strzelecka, A. Ettinger, A. W. Grenfell, T. Wittmann *et al.*, 2015 Enzymatically generated CRISPR libraries for genome labeling and screening. Dev. Cell 34: 373–378.

Lienkamp, S. S., K. Liu, C. M. Karner, T. J. Carroll, O. Ronneberger *et al.*, 2012 Vertebrate kidney tubules elongate using a planar cell polarity-dependent rosette-based mechanism of convergent extension. Nat. Genet. 44: 1382–1387.

Lyons, J. P., R. K. Miller, X. Zhou, G. Weidinger, T. Deroo *et al.*, 2009 Requirement of Wnt/β-catenin signaling in pronephric kidney development. Mech. Dev. 126: 142–159.

Moody, S. A., 1987a Fates of the blastomeres of the 16-cell stage *Xenopus* embryo. Dev. Biol. 119: 560–578.

Moody, S. A., 1987b Fates of the blastomeres of the 32-cell-stage *Xenopus* embryo. Dev. Biol. 122: 300–319.

Moody, S. A., and M. J. Kline, 1990 Segregation of fate during cleavage of frog (*Xenopus laevis*) blastomeres. Anat. Embryol. (Berl.) 182: 347–362.

Moreno-Mateos, M. A., C. E. Vejnar, J. Beaudoin, J. P. Fernandez, E. K. Mis *et al.*, 2015 CRISPRscan: designing highly efficient sgRNAs for CRISPR/Cas9 targeting *in vivo*. Nat. Methods 12: 982–988.

Naert, T., R. Colpaert, T. Van Nieuwenhuysen, D. Dimitrakopoulou, J. Leoen *et al.*, 2016 CRISPR/Cas9 mediated knockout of rb1 and rbl1 leads to rapid and penetrant retinoblastoma development in *Xenopus tropicalis*. Sci. Rep. 6: 35264.

Naert, T., T. Van Nieuwenhuysen, and K. Vleminckx, 2017 TALENs and CRISPR/Cas9 fuel genetically engineered clinically relevant *Xenopus tropicalis* tumor models. Genesis 55: 1–2.

Nakayama, T., M. B. Fish, M. Fisher, J. Oomen-Hajagos, G. H. Thomsen *et al.*, 2013 Simple and efficient CRISPR/Cas9-mediated targeted mutagenesis in *Xenopus tropicalis*. Genesis 51: 835–843.

Nieuwkoop, P. D., and J. Faber, 1994 *Normal Table of Xenopus laevis (Daudin): A Systematical & Chronological Survey of the Development from the Fertilized Egg till the End of Metamorphosis*. Garland Publishing, Inc., New York.

Omasits, U., C. H. Ahrens, S. Muller, and B. Wollscheid, 2014 Protter: interactive protein feature visualization and integration with experimental proteomic data. Bioinformatics 30: 884–886.

Rankin, S. A., J. Kormish, M. Kofron, A. Jegga, and A. M. Zorn, 2011 A gene regulatory network controlling hhex transcription in the anterior endoderm of the organizer. Dev. Biol. 351: 297–310.

Sander, J. D., P. Zaback, J. K. Joung, D. F. Voytas, and D. Dobbs, 2007 Zinc Finger Targeter (ZiFiT): an engineered zinc finger/target site design tool. Nucleic Acids Res. 35: W599–W605.

Sander, J. D., M. L. Maeder, D. Reyon, D. F. Voytas, J. K. Joung *et al.*, 2010 ZiFiT (Zinc Finger Targeter): an updated zinc finger engineering tool. Nucleic Acids Res. 38: W462–W468.

Session, A. M., Y. Uno, T. Kwon, J. A. Chapman, A. Toyoda *et al.*, 2016 Genome evolution in the allotetraploid frog *Xenopus laevis*. Nature 538: 336–343.

Shawlot, W., and R. R. Behringer, 1995 Requirement for Lim1 in head-organizer function. Nature 374: 425–430.

Shigeta, M., Y. Sakane, M. Iida, M. Suzuki, K. Kashiwagi *et al.*, 2016 Rapid and efficient analysis of gene function using CRISPR-Cas9 in *Xenopus tropicalis* founders. Genes Cells 21: 755–771.

Sive, H. L., R. M. Grainger, and R. M. Harland, 2000 *Early Development of Xenopus laevis: A Laboratory Manual*. Cold Spring Harbor Laboratory Press, Cold Spring Harbor, NY.

Taira, M., M. Jamrich, P. J. Good, and I. B. Dawid, 1992 The LIM domain-containing homeo box gene Xlim-1 is expressed specifically in the organizer region of *Xenopus* gastrula embryos. Genes Dev. 6: 356–366.

Taira, M., H. Otani, M. Jamrich, and I. B. Dawid, 1994 Expression of the LIM class homeobox gene Xlim-1 in pronephros and CNS cell lineages of *Xenopus* embryos is affected by retinoic acid and exogastrulation. Development 120: 1525–1536.

Tandon, P., F. Conlon, J. D. Furlow, and M. E. Horb, 2017 Expanding the genetic toolkit in *Xenopus*: approaches and opportunities for human disease modeling. Dev. Biol. 426: 325–335.

Tomlinson, M. L., R. A. Field, and G. N. Wheeler, 2005 *Xenopus* as a model organism in developmental chemical genetic screens. Mol. Biosyst. 1: 223–228.

Venegas-Ferrin, M., N. Sudou, M. Taira, and E. M. del Pino, 2010 Comparison of Lim1 expression in embryos of frogs with different modes of reproduction. Int. J. Dev. Biol. 54: 195–202.

Vize, P. D., E. A. Jones, and R. Pfister, 1995 Development of the *Xenopus* pronephric system. Dev. Biol. 171: 531–540.

Wang, F., Z. Shi, Y. Cui, X. Guo, Y. B. Shi *et al.*, 2015 Targeted gene disruption in *Xenopus laevis* using CRISPR/Cas9. Cell Biosci. 5: 15.

Watanabe, M., Y. Yasuoka, S. Mawaribuchi, A. Kuretani, M. Ito *et al.*, 2017 Conservatism and variability of gene expression profiles among homeologous transcription factors in *Xenopus laevis*. Dev. Biol. 426: 301–324.

Wheeler, G. N., and A. W. Brändli, 2009 Simple vertebrate models for chemical genetics and drug discovery screens: lessons from zebrafish and *Xenopus*. Dev. Dyn. 238: 1287–1308.

Yasuoka, Y., Y. Suzuki, S. Takahashi, H. Someya, N. Sudou *et al.*, 2014 Occupancy of tissue-specific cis-regulatory modules by Otx2 and TLE/Groucho for embryonic head specification. Nat. Commun. 5: 4322.

Communicating editor: O. Hobert